Different rules for binocular combination of luminance in cortical and subcortical pathways

Federico G. Segala, Aurelio Bruno, Alex R. Wade & Daniel H. Baker (+Myat? +Joel?)

2022-09-26

Abstract

Introduction

Binocular combination provides a higher visual sensitivity than monocular viewing. This superiority is known as binocular summation and is defined by the binocular summation ratio (BSR), which was originally believed to be around $\sqrt{2}$ (≈ 1.4) for grating stimuli at detection threshold (Campbell and Green, 1965). In other words, a monocular stimulus can elicit the same response as a binocular stimulus if it has a contrast that is 1.4 times higher. This led Legge to develop a widely accepted explanation that used quadratic summation to describe binocular combination (Legge, 1984): monocular signals from the right (R) and the left (L) eyes are squared before being summed together and the binocular response (B) is given by the square root of the output ($B = \sqrt{R^2 + L^2}$, when R and L are equal to 1, the output is $\sqrt{2}$). However, subsequent research has shown that these explanations are not fully adequate to account for binocular summation. Both of these accounts constitute single channel models, and this type of model has been shown to not being able to account for contrast detection in the presence of noise (Anderson and Movshon, 1989). Moreover, more recent research has shown that the summation ratio can vary greatly between $\sqrt{2}$ and 2 depending on factors such as the spatial and temporal frequency of a stimulus or the sensitivity difference between the eyes (Baker et al., 2018). These observations led to the development of multistage gain control models, which combine binocular summation and interocular suppression, and can account for contrast matching, detection and discrimination for spatial contrast (Ding and Sperling, 2006; Meese et al., 2006). In general, it seems that the mechanisms behind binocular combination have been thoroughly studied, as have been the anatomical pathways behind it: light enters the eye though the pupil and signals are sent from the left and right retinae to the primary visual cortex, remaining anatomically isolated while passing through the lateral geniculate nucleus (LGN) until they reach V1, where they are binocularly combined (Purves et al., 2008). However, there is an eye component that is often underestimated in its role to determine the quality of visual information: the pupil. The pupils are openings found in the centre of the eyes that appear to be black and allow light to enter the eyes. Their size determines how much light will reach the retina and it is usually determined by the ambient levels of light: in brightness the pupils will constrict and in darkness they will dilate. This is known as the pupillary light response (PLR). The anatomical pathways that regulate this response are well understood and are very clearly and extensively described in the literature (Angée et al., 2021; Mathôt, 2018; McDougal and Gamlin, 2010; Wang and Munoz, 2015). However, they are anatomically distinct from the LGN-V1 pathway meaning that binocular combination occurs separately in anatomically distinct pathways. Given this, not much is known about the computational processes behind the PLR except for some evidence of binocular interaction. The presence of a consensual response in one eye when the other is being stimulated, and the presence of convergence (one pupil responds to illumination in either retina) and divergence (both pupils respond to illumination of one retina) (Wyatt and Musselman, 1981) are evidence of this binocular interaction. With this in mind we designed an experiment that simultaneously recorded electrophysiological and pupillometric responses to investigate the combination of flickering light

signals in both the visual cortex and the pupils. The results should offer new insight about basic neural circuits and information on how they might be affected in clinical disorders of vision (e.g. amblyopia). Based on previous literature, we expected to find a non-linear combination of the responses in visual cortex, as described by the gain control mechanisms, and a more linear combination of the responses and a greater binocular response at the level of the pupils. To follow up on the results that we obtained, we decided to perform a contrast matching experiment to investigate whether perception of flickering light is consistent with the results observed in the cortical pathways (visual cortex) or the subcortical pathways (pupils). Matching is a paradigm in which the perceived brightness of a standard stimulus is matched to that of a target stimulus. In the latter, the interocular ratios of luminance are varied to obtain an equibrightness curve. Previous literature has used this paradigm to investigate the binocular fusion of static stimuli and the temporal combination of spatial flickering of spatial increments (a bright target on a dark background) and decrements (a dark target on a bright background) (Anstis and Ho, 1998; Levelt, 1965). For spatial increments, it was found that binocular fusion seems to follow approximately linear combination rules. This means that, for a monocular stimulus to elicit the same response as a binocular stimulus, the former needs to have twice the signal of the latter. On the other hand, spatial decrements follow a winner-takes-all pattern. This means that the observer is seeing what the eye that is receiving the strongest signal is seeing. Our experiment used different stimuli than the ones used by Anstis and Ho: in the binocular fusion experiment, their stimuli were not flickering and, in the flicker experiment, they were always shown in both eyes. In our experiment, in some conditions, the flicker was shown to only one eye. Moreover, they were looking at the temporal fusion of the flicker while we focussed on the binocular fusion of the flicker. Based on this and on the results from our first experiment, we expected to find a near linear summation of the responses.

Methods

Participants

Apparatus & Stimuli

Procedure

Data analysis

Results

Experiment 1

Figure @ref(fig:pupildata)a

Experiment 2

Experiment 3

Computational modelling

Table 1: Summary of median parameter values.

Data set	Z	k	w	Rmax
Pupillometry	2.45	0.01	0.67	0.00024

Data set	Z	k	w	Rmax
EEG 1F	2.78	0.15	0.03	0.00262
EEG 2F	2.31	0.06	0.01	0.00407
Matching	0.56	7.96	0.05	-

Discussion

References

Anderson PA, Movshon JA. 1989. Binocular combination of contrast signals. *Vision Res* **29**:1115–32. doi:10.1016/0042-6989(89)90060-6

Angée C, Nedelec B, Erjavec E, Rozet J-M, Fares Taie L. 2021. Congenital microcoria: Clinical features and molecular genetics. *Genes (Basel)* **12**. doi:10.3390/genes12050624

Anstis S, Ho A. 1998. Nonlinear combination of luminance excursions during flicker, simultaneous contrast, afterimages and binocular fusion. *Vision Res* **38**:523–39. doi:10.1016/s0042-6989(97)00167-3

Baker DH, Lygo FA, Meese TS, Georgeson MA. 2018. Binocular summation revisited: Beyond $\sqrt{2}$. *Psychol Bull* **144**:1186–1199. doi:10.1037/bul0000163

Campbell FW, Green DG. 1965. Monocular versus binocular visual acuity. *Nature* **208**:191–2. doi:10.1038/208191a0

Ding J, Sperling G. 2006. A gain-control theory of binocular combination. *Proc Natl Acad Sci U S A* **103**:1141–6. doi:10.1073/pnas.0509629103

Legge GE. 1984. Binocular contrast summation–ii. Quadratic summation. *Vision Res* **24**:385–94. doi:10.1016/0042-6989(84)90064-6

Levelt WJ. 1965. BINOCULAR brightness averaging and contour information. *Br J Psychol* **56**:1–13. doi:10.1111/j.2044-8295.1965.tb00939.x

Mathôt S. 2018. Pupillometry: Psychology, physiology, and function. *J Cogn* **1**:16. doi:10.5334/joc.18

McDougal DH, Gamlin PD. 2010. The influence of intrinsically-photosensitive retinal ganglion cells on the spectral sensitivity and response dynamics of the human pupillary light reflex. *Vision Res* **50**:72–87. doi:10.1016/j.visres.2009.10.012

Meese TS, Georgeson MA, Baker DH. 2006. Binocular contrast vision at and above threshold. *J Vis* **6**:1224–43. doi:10.1167/6.11.7

Purves D, Brannon EM, Cabeza R, LaBar KS, Huettel SA, Platt ML, Woldorff MG. 2008. Principles of Cognitive Neuroscience. Oxford University Press, Incorporated.

Wang C-A, Munoz DP. 2015. A circuit for pupil orienting responses: Implications for cognitive modulation of pupil size. *Curr Opin Neurobiol* **33**:134–40. doi:10.1016/j.conb.2015.03.018

Wyatt HJ, Musselman JF. 1981. Pupillary light reflex in humans: Evidence for an unbalanced pathway from nasal retina, and for signal cancellation in brainstem. *Vision Res* **21**:513–25. doi:10.1016/0042-6989(81)90097-3

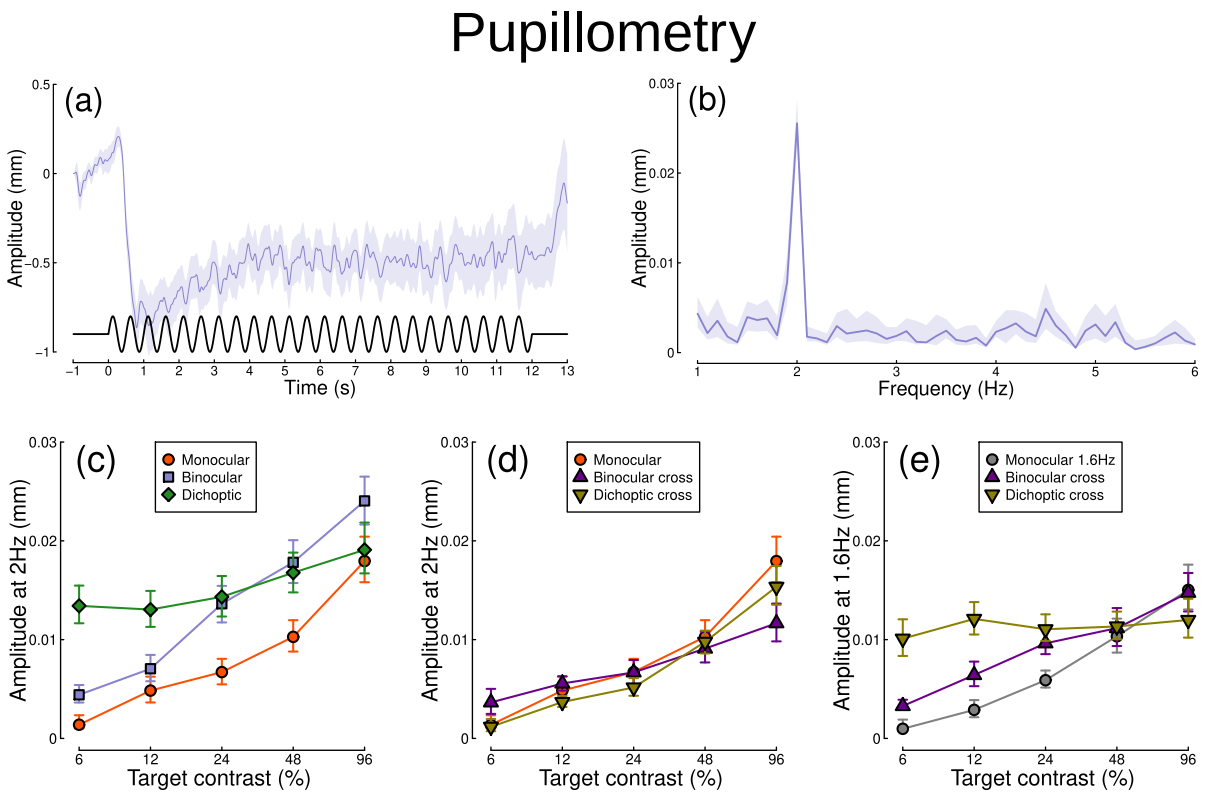

Figure 1: Summary of pupillometry results for N=30 participants. Panel (a) shows a group average waveform for binocular presentation (low pass filtered at 5Hz), with the driving signal plotted at the foot. Panel (b) shows the average Fourier spectrum. Panels (c,d) show contrast response functions at 2Hz for different conditions. Panel (e) shows contrast response functions at 1.6Hz for three conditions. Shaded regions and error bars indicate bootstrapped standard errors.

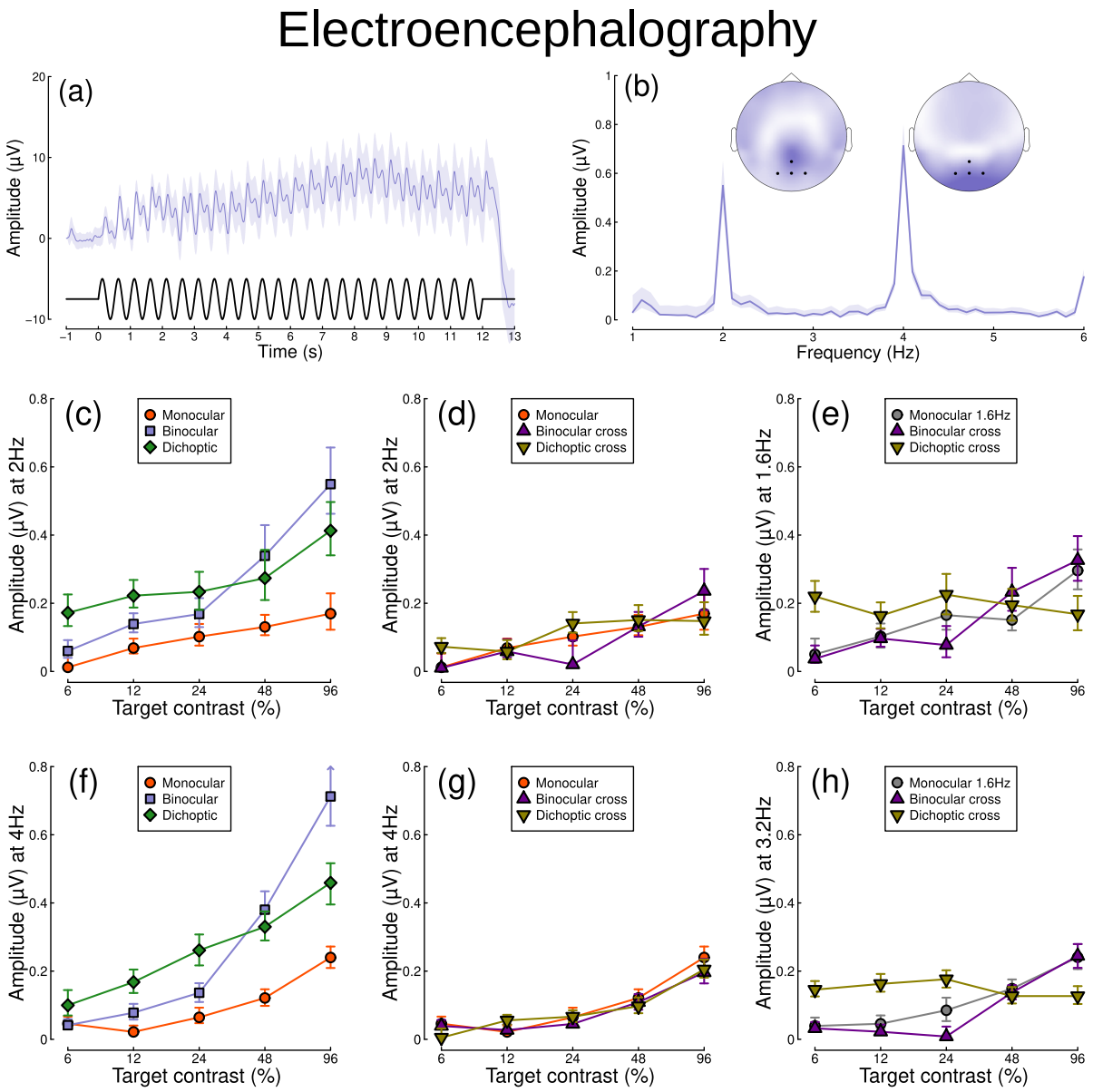

Figure 2: Summary of EEG results for N=30 participants. Panel (a) shows a group average waveform for binocular presentation (low pass filtered at 5Hz), with the driving signal plotted at the foot. Panel (b) shows the average Fourier spectrum, and inset scalp distributions. Black dots on the scalp plots indicate electrodes Oz, POz, O1 and O2. Panels (c,d) show contrast response functions at 2Hz for different conditions. Panel (e) shows contrast response functions at 1.6Hz for three conditions. Panels (f-h) are in the same format but for the second harmonic responses. Shaded regions and error bars indicate bootstrapped standard errors.

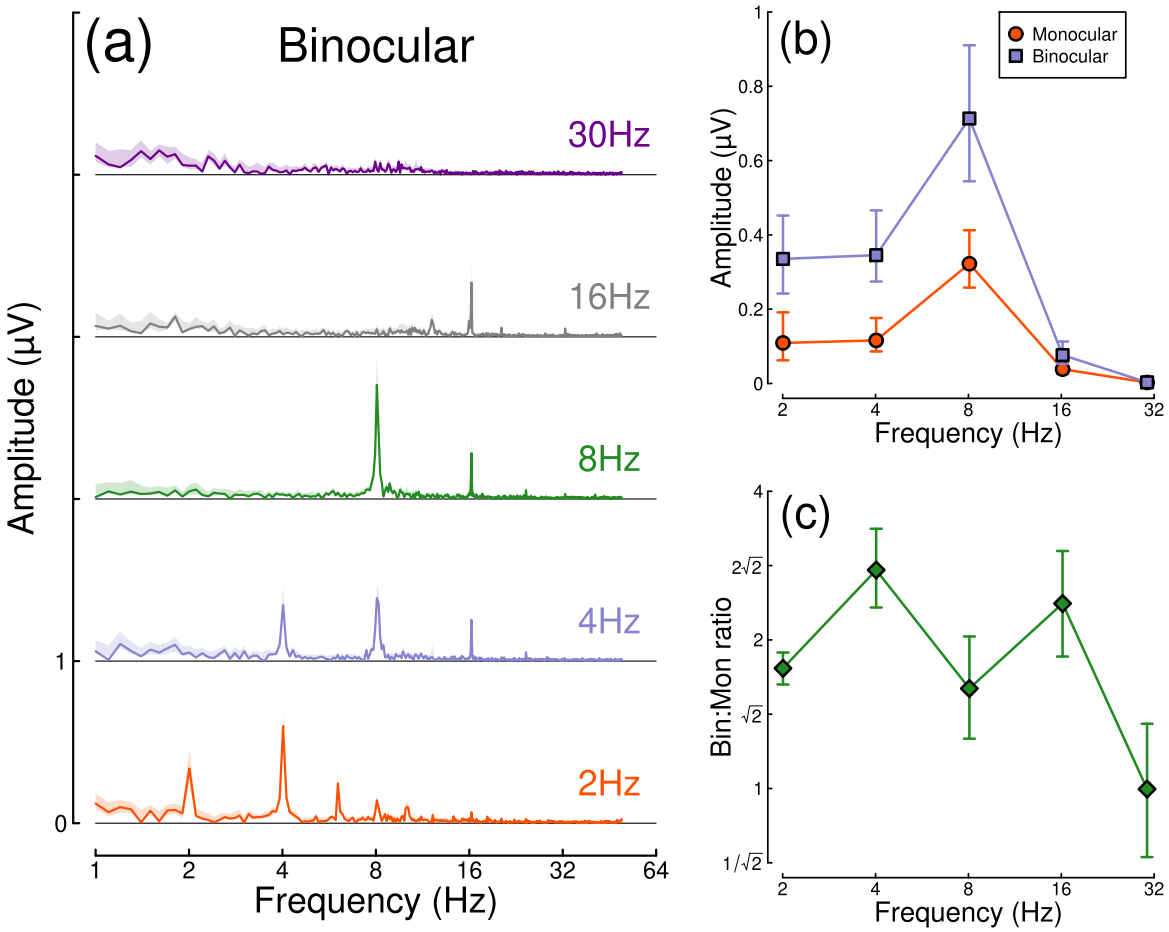

Figure 3: Binocular facilitation at different temporal frequencies. Panel (a) shows Fourier spectra for responses to binocular flicker at 5 different frequencies (offset vertically for clarity). Panel (b) shows the response at each stimulation frequency for monocular (red) and binocular (blue) presentation. Panel (c) shows the ratio of binocular to monocular responses. Error bars and shaded regions indicate bootstrapped standard errors across N=12 participants.

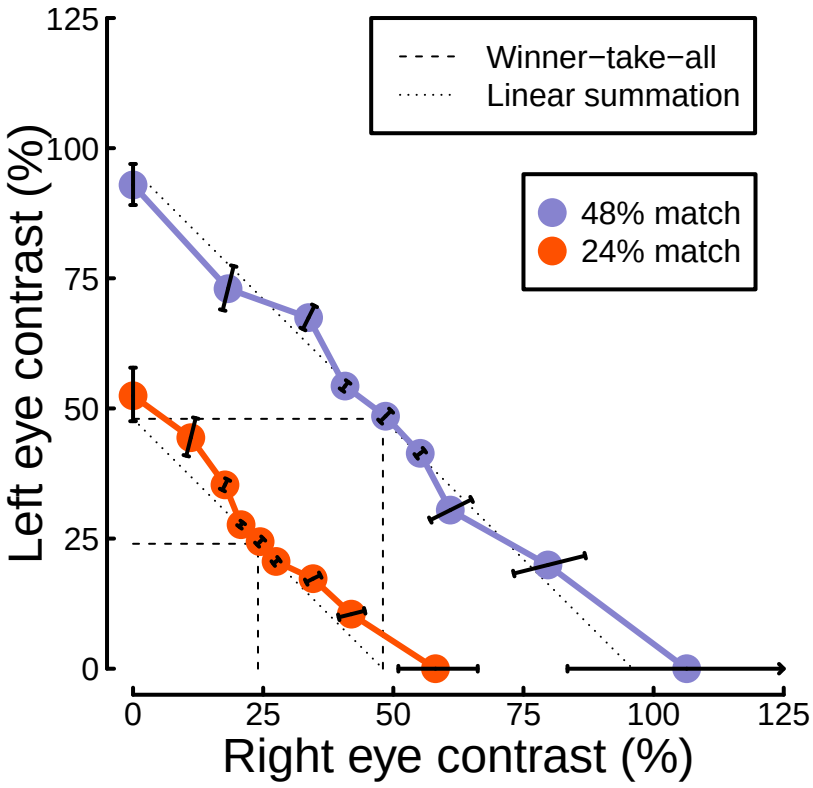

Figure 4: Contrast matching functions. Dotted and dashed lines are predictions of canonical summation models with a linear exponent (dotted) or an infinite exponent (dashed). Error bars indicate the standard error across participants (N=10), and are constrained along radial lines converging at the origin.

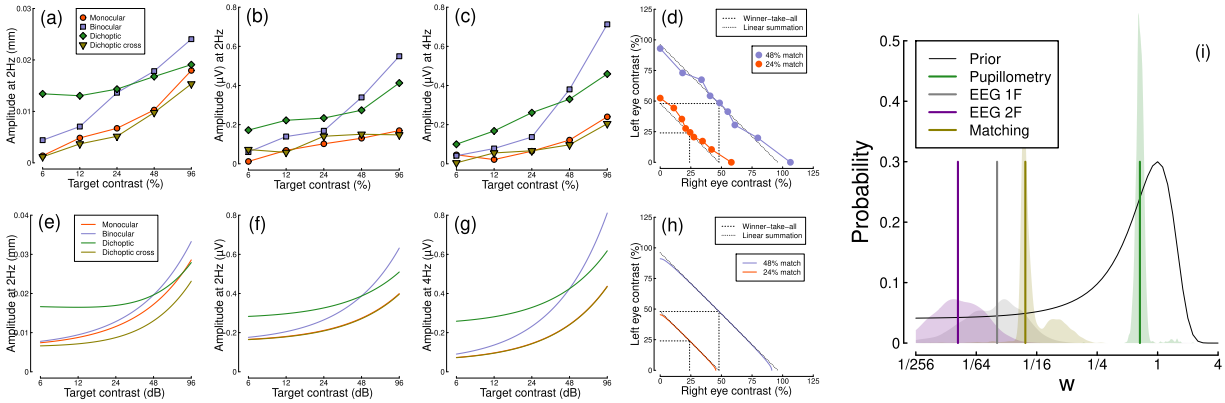

Figure 5: Summary of computational modelling. Panels (a-d) show model behaviour for our four main data set, pupillometry (a), first harmonic EEG responses (b), second harmonic EEG responses (c) and contrast matching (d). Panel (e) shows the posterior probability distributions of the interocular suppression parameter for each of the four model fits. The pupillometry distribution (green) is centred about a substantially higher suppressive weight than for the other data types (note the logarithmic x-axis). The black curve shows the (scaled) prior distribution for the weight parameter.